



# Bearing Capacity of Steel Square Tubular Column I-Shaped Beam Joints Connected by New Elliptical One-Sided Bolts

Weitong Yi<sup>1</sup> · Lingxiao Zuo<sup>1</sup> · Tianxi Chen<sup>1</sup> · Mei Wang<sup>2</sup> · Hailin Sun<sup>3</sup> · Lei Zhu<sup>1</sup> · Xi Chen<sup>4</sup>

Received: 14 December 2021 / Accepted: 8 September 2022 / Published online: 7 October 2022  
© Korean Society of Steel Construction 2022

## Abstract

A new elliptical one-sided bolt was applied for connection of the steel square tubular column and the I-shaped beam joint. This new bolt is simple in structure and easy to install. Besides, as the bolt head and bolt hole are both elliptical, the new one is quite different from the traditional circular bolts lacking bending performance studies of the joint. Therefore, experiments and finite element analysis on ultimate bearing capacity of the joint were conducted, monotonic static loading of six joint specimens were tested, and the moment-rotation curves were obtained in this study. The effects of various factors such as axial load ratio and bolt size on bearing capacity were analyzed. Finite element simulation was carried out, and it fitted tests well. Both tests and simulation showed that failure mode of joints is firstly yielding at the endplate. The larger the bolt size, the better the joint ultimate bearing capacity can be enhanced. The M16 group indicated a pattern that the larger axial load on column, the less of ultimate bearing capacity of the joint. However, the M20 group comes to a different pattern which contradicts the assumption, thus further studies are needed in this regard.

**Keywords** New elliptical one-sided bolt · Steel square tubular column and I-shaped beam joint · Ultimate capacity · Moment–angle curves

## 1 Introduction

Traditional steel frames mostly adopt I-shaped columns and I-shaped beams, and the moments of inertia of the two main axis directions of an I-shaped column are significantly different, resulting in the poor bending resistance in the weak axis direction (Wardenier, 2002). In contrast, when the section of

columns is square tubular, the moments of inertia of the two main axis directions are identical, which indicates a better bending performance than an I-shape column (Ridley-Ellis, 1998). However, the disadvantage of a steel square tubular column is the closed cross section, which is nearly impossible to install traditional bolts due to the narrow space inside. Therefore, one-sided bolts, which can be installed and fastened unilaterally, are increasingly applied in the connection of steel tubular column and I-shaped beams.

Since the 1990s, a variety of one-sided bolts for connecting steel members have been developed. The BOM, HSBB and Ultra-Twist bolts are 3 kinds of unilateral fasteners manufactured by Huck International in US (Korol et al., 1993; Mourad et al., 1996). These bolts require a high degree of manufacturing precision and therefore the processing cost is higher. The deformed parts of bolts may be damaged prematurely under tension, which limits the tensile capacity (Ghobarah et al., 1996). The Flowdrill technology, developed by Dutch company Flowdrill BV, is a relatively new technology for hot drilling, for which steel members are tapping firstly, then the conventional bolts without tightening the nut are available for installation (France et al., 1999a, 1999b). Hollo-bolt, developed

✉ Lei Zhu  
zhulei@bucea.edu.cn

<sup>1</sup> Beijing Advanced Innovation Center for Future Urban Design, School of Civil and Transportation Engineering, Beijing Higher Institution Engineering Research Center of Structural Engineering and New Materials, Beijing Key Laboratory of Functional Materials for Building Structure and Environment Remediation, Beijing University of Civil Engineering and Architecture, Beijing, China  
<sup>2</sup> Institute of Science and Technology Development, Beijing University of Civil Engineering and Architecture, Beijing, China  
<sup>3</sup> China Architecture Design and Research Group, Beijing, China  
<sup>4</sup> School of Humanity and Law, Beijing University of Civil Engineering and Architecture, Beijing, China

by Lindapter International of the UK, is inserted into a pre-drilled hole, and tightened via a torque spanner on the head side of the bolt. The applied torque moves the cone towards the outside of the joint, which expands the leg and creates a solid fixing that prevents the bolt from pulling out (Thai & Uy, 2015; Wang & Wang, 2016). ONESIDE bolts of Ajax Engineered Fasteners in Australia is relatively new. It contains several parts and requires a special tool for installation. It relies on a special collapsible washer that is folded before insertion and unfolded with a special tool after installation (Lee et al., 2010). The Blind Bolt from Blindbolt Company in UK allows an one-sided installation by means of retractable locking anchors. To install the bolt, the locking anchor is retracted and the end of the bolt inserted into the clearance hole, then the locking anchor is loosened to allow the bolt to be tightened (Satasivam & Bai, 2014; Wu et al., 2014). Tongji University developed a split one-sided bolt that can well meet the force requirements of friction-type high-strength bolts (Wang et al., 2018a, 2018b).

For research involved in mechanical properties of beam-column joints, Pitrakkos and Tizani (2013) presented a new kind of one-sided bolt which is an improvement of EHB, and for mechanical performance of joints, the preloading level of the component was quantified and its complete nonlinear load–displacement response was measured. Lee et al. (2010) carried out joint tests of Ajax one-sided bolt under monotone tension and compression, it was found to be semi-rigid under normal service conditions of the joint. Elghazouli (2009) explored experimental performance of blind bolt angle steel connection between I-beam and steel tubular column, as well

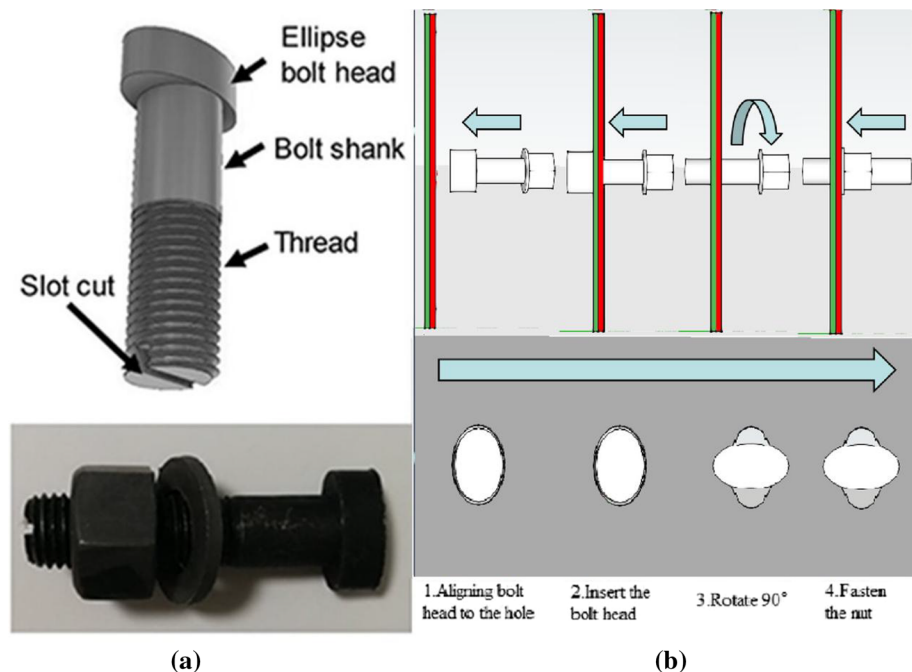
as the simplified calculation method of initial stiffness and yield parameters of member joints.

For research involved in dynamical responses of frame structure, John et al. (2020a, 2020b, 2020c, 2021) proposed a new kind of slider device. This novel slider was connected by a rod, where screw threads were made up at both side of the rod so that the slider could be tightened by nuts. Several rubber blocks were fixed inside the slider as for aseismic. During several vibration table tests about scaled storey structure, it was proved that the slider has well energy-dissipating capacity, as well structural displacement can be reduced effectively.

Most current one-sided bolts are complex in structure and inconvenient for installation, some of them require special equipment and technology. It is necessary to develop a new type of one-sided bolts which are easier to install and more cost-saving, helping for a wider application of the one-sided bolts in steel tubular components.

A new type of one-sided bolt is proposed as Fig. 1a. Figure 1b is the method of installation (Wan et al., 2020). The innovation of the bolt is embodied in the shape of the head, which is elliptical instead of the traditional circular. By inserting the elliptical bolt head into the bolt hole reserved in the connection member and rotating it by 90 degrees, the bolt head can be blocked by the inner wall of the member, then the bolt can be tightened by the nut outside. Another innovation about this one-sided bolt is at the end of the bolt rod, which has a cut-out parallel to the direction of the long axis, thus the posture of the bolt head can be made clear from the outside during the installation, to ensure the correctness of the one-sided bolt installation. Given that both

**Fig. 1** Proposed one-sided bolt and installation method



bolt head and hole are elliptical, different from the traditional circular bolt, it will lead to differences in ultimate bearing capacity of steel square tubular column and I-shaped beam joints, which needs to be further studied. This research will explore bearing capacity of the joint based on static behavior tests and correspond finite element analysis.

## 2 Test Approach

### 2.1 Test System and Specimens Design

The apparatus of joint tests is shown as Fig. 2a, including an actuator for axial load which can reach in 6000 kN, another actuator up to 1000 kN for beam loading, the ground beam, and the rigid reaction frame to ensure test safety. Figure 2 is the site layout of the test. For actuators adopted in the tests, both data of force and displacement can be recorded by IMP acquisition system in real time.

For specimens of the tests, new elliptical one-sided bolts were applied to connect the steel square tubular column and I-shaped beam. Monotonic loads were applied to the end of the beam to get the ultimate bearing capacity, as well as the moment-rotation curves of the beam. 6 specimens were designed which were divided into two groups, one was connected by M16 bolts, while the other by M20. Each group contained three specimens under different axial loads to the column, for the axial load ratio were 0.0, 0.2 and 0.4.

According to the size of the test system, the length of steel square tubular column was set as 3000 mm, and 2700 mm for I-shaped beam. The section size of steel square tubular columns was selected according to 1/12 of the length as 300 mm, and the thickness was set as 12 mm. For I-shaped beams, section size was set as

294 mm × 200 mm × 8 mm × 12 mm. To meet the demand of bolt connection between beam and column, one end of the I-shaped beam should be welded with overhanging endplate. The width of endplates was equal to the column which was 300 mm, and the length was designed as follows:

$$h_d = h_b + 2(e_f + c)$$

$h_d$ —The height of I-shaped beam (mm).

$e_f$ —Distance between the outermost row of bolts and the outer edge of the flange of I-shaped beam (mm).

$c$ —Distance from the outermost row of bolts to the edge of the end plate (mm).

Based on this, the length of the endplate was set as 540 mm. According to the current experiments, when the thickness of the endplate increases in a certain range, the flexural bearing capacity of joints can be improved. As Technical specification of lightweight steel and lightweight concrete structures (JGJ383-2010, 2010) indicated, when the type of endplate is overhanging, the thickness should not be less than 16 mm. Therefore, the endplate thickness valued 16 mm.

For bolts in tests, the ratio of long to short axis was set as 1.7, according to the previous research (Wan et al., 2020) about the best shear performance of bolts. Bolt holes should be reserved on columns and endplates according to the bolt positions, which shape were also elliptical. In these tests, beam-column were connected by two rows of bolts, and each row is equipped with four. In order to facilitate the installation of the new type of elliptical one-sided bolts, the hole aperture should be slightly larger than the size of bolt head. For M20 cases, the hole aperture should be increased by 2 mm based on

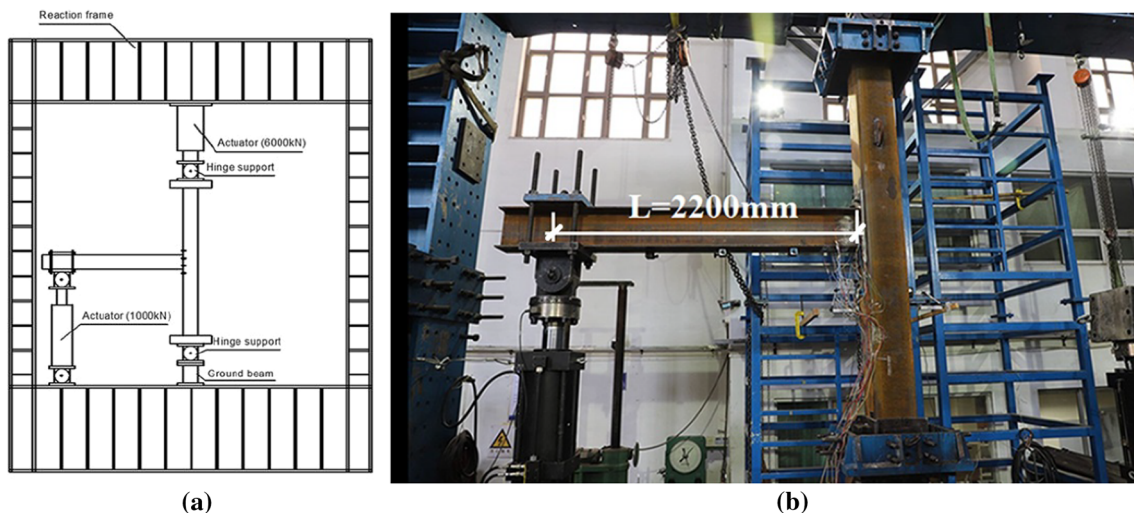


Fig. 2 Test apparatus

the diameter of the bolt, for M16 cases, the increase was 1 mm. All the sizes of the specimens are summarized as Table 1.

### 2.2 Material Properties

Bolts were adopted 10.9 class. For material besides bolts, specimens which in shape of dog-bone for material property tests were derived from the flange of I-shaped steel beam, web of the beam, steel square tubular column and endplate. Tests were referred to code (GB/T228.1-2010, 2010), as average values of material property tests were taken to represent the material property parameters, as shown in Table 2.

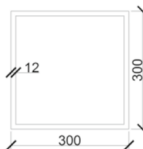
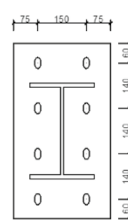
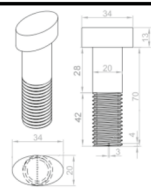
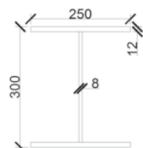
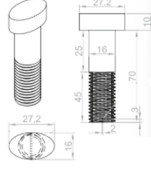
### 2.3 Loads Application

Loads included preload of bolts and load at the end of the beam. For bolts preload, it was work out by the following formula:

$$F_{pb} = k \cdot f_{yb} \cdot A_{sb} = \frac{k \cdot f_{yb} \cdot \pi \cdot d_b^2}{4}$$

- $F_{pb}$ —Pretension of the bolt
- $k$ —Pretension coefficient. For bolts in tests, it was valued by 0.2
- $f_{yb}$ —Yield stress of the bolt which was valued by 900 MPa
- $d_b$ —Diameter of the bolt

**Table 1** Specimens size

Specimen number	Beam and column size	Endplate size	bolt size (mm)	Axial load ratio
	(mm)	(mm)		
SJ-1				0
SJ-2				0.2
SJ-3				0.4
SJ-4		Beam length: 2700 Column length: 3000 Endplate thickness: 16		0
SJ-5				0.2
SJ-6				0.4

**Table 2** Material properties

Elastic properties	Yield strength /MPa		Tensile strength /MPa		Elastic modulus /GPa	Elongation/%
Flange of I-shaped beam	293		429		198	33.5
Web of I-shaped beam	263		416		187	42.1
Steel square tubular column	335		504		190	28.6
Endplate	254		435		185	38.9
Plastic properties	Stress/MPa	Stress/MPa	Stress/MPa	Stress/MPa	Stress/MPa	Stress/MPa
	Strain	Strain	Strain	Strain	Strain	Strain
Flange	293	400	426	429	420	290
	0.006	0.05	0.1	0.15	0.25	0.31
Web	263	343	390	416	414	294
	0.023	0.05	0.1	0.23	0.35	0.43
Column	335	447	498	504	500	339
	0.016	0.05	0.1	0.2	0.25	0.31
Endplate	254	365	415	435	402	332
	0.017	0.05	0.1	0.2	0.35	0.405

Therefore, the preload of M16 and M20 bolts were set 36.2 kN and 56.5 kN. The axial load of column was applied by multiplying with yield stress of column to a ratio of 0.2 and 0.4, which corresponded to 926 kN and 1852 kN. The load of beam displacement control was applied with a speed of 20 mm/min. When the component was deformed significantly or damaged, the experiment terminated.

### 3 Test Results

#### 3.1 Test Phenomenon

When a steel square tubular column is subjected to axial pressure and the actuator is pushed upwards at the end of the beam, there are four possible deformation damage scenarios in joints: (1) yield of column wall; (2) yield of beam shear; (3) yield of endplate; (4) yield of one-sided bolts and even bolts pulled off.

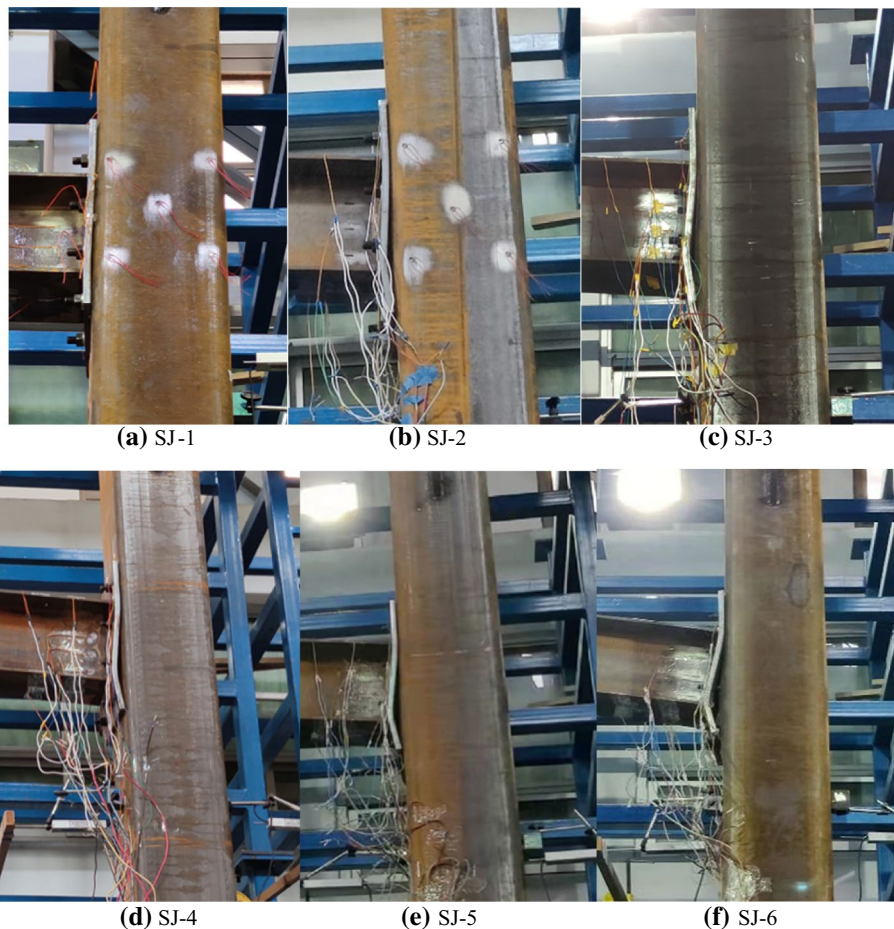
In specimen SJ-1, because no axial pressure was applied, safety considerations were taken to prevent the specimen from being detached from the test instrument as a whole. The loading was stopped just as the specimen entered the

yielding phase, at which point the beam end displacement was 86.74 mm. In this group of tests, it could be observed that the endplate had slight bending deformation at the position of the lower flange of the beam, minor deformation of the bolt holes of the steel square tubular column has occurred outside and there was no obvious deformation of the beam, column and bolts. The deformation of the specimen is shown in Fig. 3a.

In specimen SJ-2, the actuator displacement range was considered without taking into account the fact that the actuator had been pushed out by approximately 340 mm in the initial state, resulting in the beam end being displaced to 163 mm during the experiment, when the actuator range was not sufficient to force the beam to stop. At the end of the test, the deformation of the specimen was found to be significantly warped at the endplate, bulging at the bolt holes on the tensioned side of the column wall and slight slippage of the single side bolts, with no significant deformation of the flange of the I-shaped steel beam. The deformation of the specimen is shown in Fig. 3b.

In specimen SJ-3, the beam end displacement was loaded to 290.71 mm when the vertical load value measured at the beam end loading point stopped increasing and the test was

Fig. 3 Specimen deformation diagram



completed. By observing the deformation of the joint, it was found that the distance between the second row of bolts of the externally endplate and the steel square tubular column was widely stretched, resulting in a gap of approximately 6 mm in width, with a slight slippage of the one-sided bolts along the column wall, and an obvious bulging phenomenon at the bolt holes of the column wall. The joint damage was judged to be caused by a large plastic deformation between the endplate and the column wall. The deformation of the specimen is shown in Fig. 3c.

In specimen SJ-4, the load at the end of the beam ceased to increase when the load reached 195.75 mm and the curve in the data acquisition device showed a decreasing trend. It was observed that the damage was mainly in the form of excessive plastic deformation of the endplate and bulging damage to the wall of the steel square tubular column. The deformation of the specimen is shown in Fig. 3d.

In specimen SJ-5, when the displacement at the loading point of the beam end increased to 264 mm, the load data collected at the end of the beam stopped increasing and the

deformation of the beam-column joint with the endplate and the steel square tubular column continued to increase. Considering the safety of the test, the loading was stopped. At the end of the test, the deformation of the beam-column joint was observed. There was a significant bending deformation at the second row of bolts on the tensioned side of the endplate, and the out-of-plane bending of the steel square tubular column wall was also evident at the second row of bolts. The two rows of single-sided bolts on the tensioned side had slipped to varying degrees: the first row of bolts was found to be slightly bent after dismantling the joint, while the second row of bolt heads had shear deformation. The bolt holes were extruded and deformed. In summary, the damage pattern of the joint was the flexure of the endplate, bulging of the steel square tubular column and bending yield of the bolts. The deformation of the specimen is shown in Fig. 3e. The one-sided bolt deformation is shown in Fig. 4a.

In specimen SJ-6, when the beam end displacement was loaded to 369 mm, the beam-column joint suddenly made a metal fracture sound and the curve plotted on the data

Fig. 4 Bolt deformation diagram

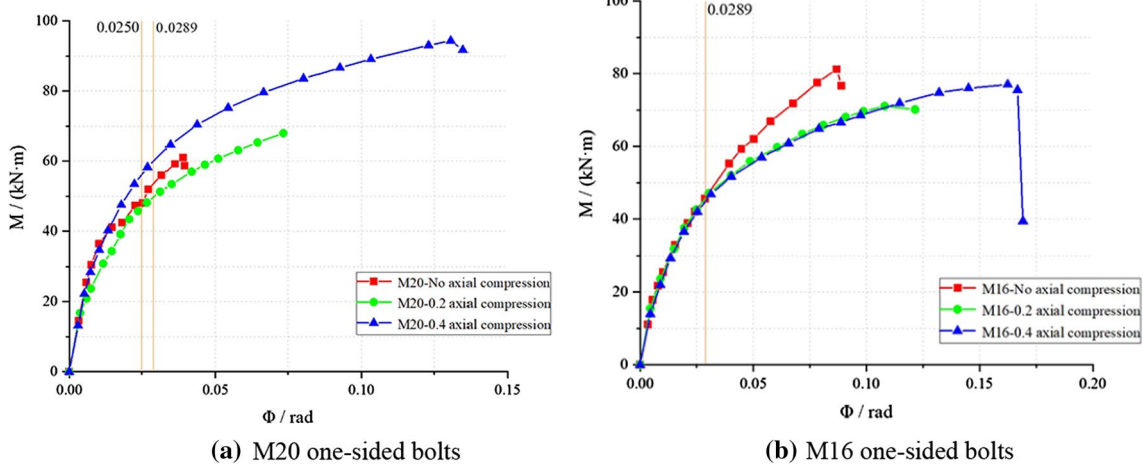
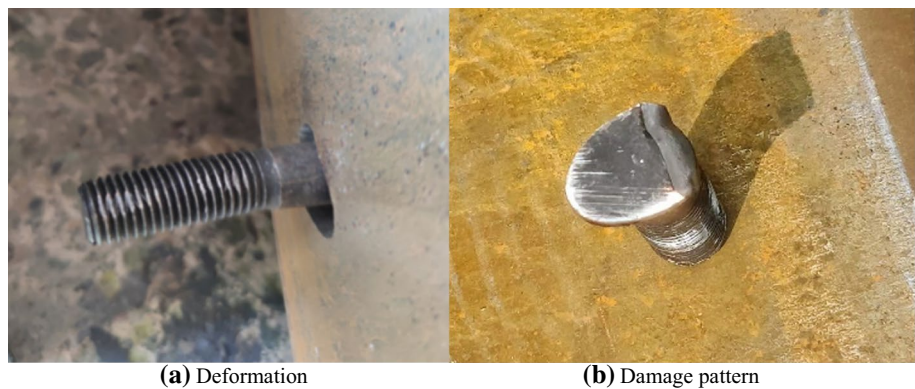
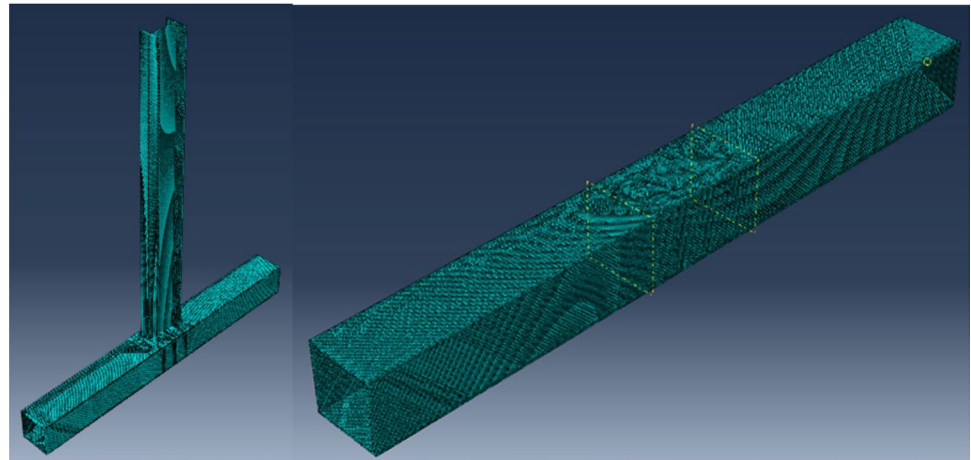


Fig. 5 Bending moment-rotation curve

acquisition side showed a steep drop, indicating that the beam-column joint had been damaged and the test was over. After dismantling the beam-column joint, it was observed

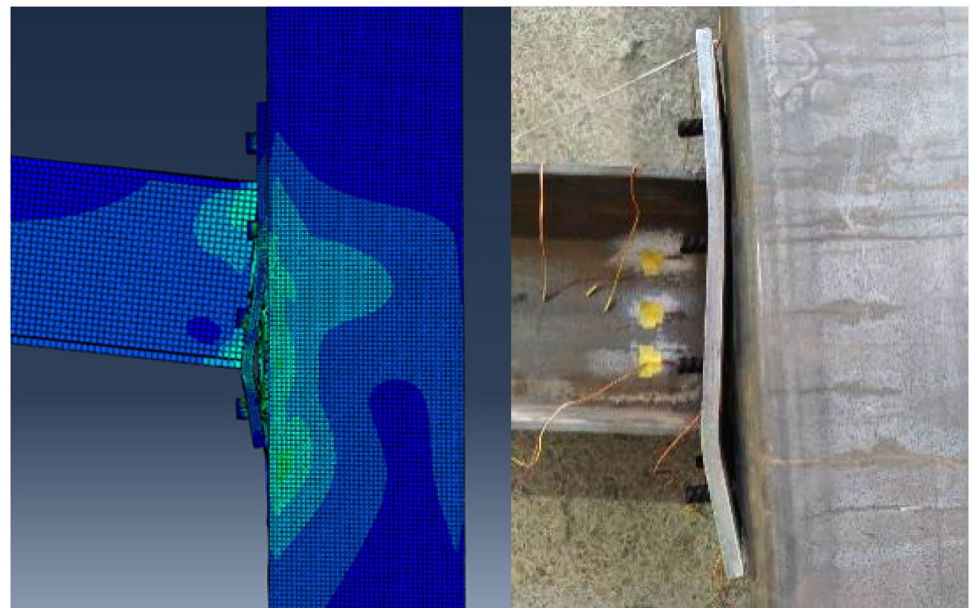
that the final fracture of the specimen was caused by shear damages to the elliptical bolt heads of the first and the second rows of one-sided bolts on the tension side, with the

**Fig. 6** Finite element model and results



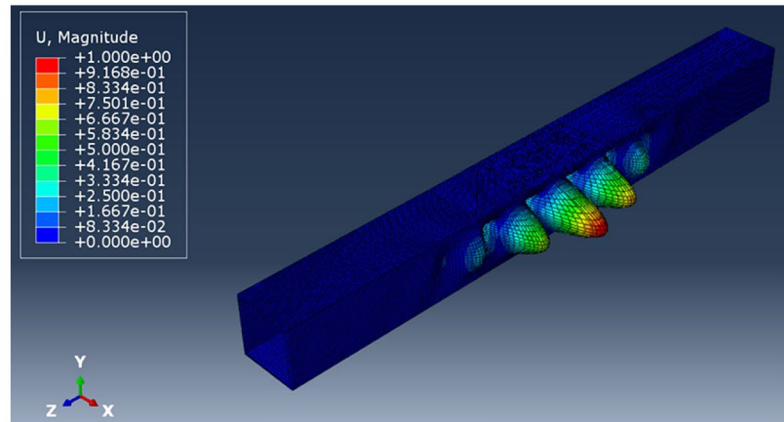
**(a)** Joint model

**(b)** Model of buckle analysis



**(c)** Stress pattern and deformation

**(d)** Test deformation



**(e)** First order mode in buckle analysis

one-sided bolts fracturing from the bolt heads under shear. At the bolt holes on the tensile side of the steel square tubular column wall, the bolt holes were partially pulled apart and small cracks appeared due to the slippage of the one-sided bolts and the large deformation of the bolt heads and bolt holes under extrusion. Endplates showed tiny cracks at the edge of the second row of bolt holes on the tensioned side, and the bending deformation was more serious. The deformation of the specimen is shown in Fig. 3f. The shear failure diagram of the one-sided bolt is shown in Fig. 4b.

### 3.2 Moment-Rotation Curves

The moment-rotation curves of tests could be derived from IMP collection, as the bending moment of the beam was calculated by the product of the beam load to the distance between the loading point and the outer wall of the column, and for rotation it was defined as the division of the displacement variation of actuator to the distance between loading point and outer wall of the column. The distance between the loading point and the outer wall of the column is shown as Fig. 2b, for it is smaller than the beam length. The curves of 6 tests are shown as Fig. 5, as Fig. 5a is the group of M20, Fig. 5b is the group of M16.

Given that the moment-rotation curve has been rising and there is no peak point, the ultimate load cannot be determined directly. Therefore, it is necessary to manually specify a judgment basis for ultimate load. In this paper, the method is used to compare the CIDECT method (1986) with the Yura method (1980), and the smaller extreme limit is selected as the ultimate load. It follows that only the SJ-6 specimen reaches the ultimate load at the rotation of 0.0250, the other specimens reach the ultimate load at the rotation of 0.0289.

Based on the bending moment-rotation curve we can see that the change in axial load ratio has essentially no effect on the ultimate load of the joint until the ultimate load is reached in the M16 one-sided bolted joint test; in the M20 one-sided bolt tests, when the axial load ratio reached 0.4, the ultimate load is even greater than at 0.2 axial load ratio. This was contrary to our expectation that the ultimate load becomes smaller when the axial load ratio increases, so we carried out finite element analyses of six separate sets of joints to analyze the effect of axial load ratio and bolt size on the beam-column joints.

## 4 Finite Element Analysis

### 4.1 Finite Element Modeling

Groups of test joints were simulated by ABAQUS. All components of joints had been modeled in solid elements, and 8-node linearly reduced integral solid units (C3D8R) were

adopted shown as Fig. 6a, which the total number of elements were approximately 168,000. Another model which only contains steel tubular column as Fig. 6b was established for buckle analysis, as the first order model was extracted for initial imperfection. Three analysis steps were defined, for the first step was the application of bolts pretension with initial imperfection added on column, the second for column axial load, and the last for load at the end of the beam. Non-linear function was selected for simulation, and in order to get a better convergence of results, automatic stabilization was defined in all analysis steps by specifying dissipated energy fraction. The first was valued by 0.001, and the rest by 0.0005. All steps were defined adaptive stabilization with maximum ratio of stabilization to strain energy as 0.05.

The selection of the constitutive relationship was a multi-linear model according to material property tests, for elastic modulus referred to Table 2, Poisson ratio valued 0.3, and plastic parameters are shown in Table 3. Surface-to-surface contacts were defined between the bolt nuts and the endplate, the endplate and the outer wall of the column, the bolt heads and the inner wall of the column, the bolt shanks and the bolt holes, with a hard contact in normal direction and friction in tangential direction. According to the Chinese (Technical, 2011), the friction coefficients were all taken as 0.3. Tie contacts were defined between the I-shaped beam and the endplate, as well as the bolt nuts and the bolt shanks.

Bolt pretension was added on the cut surface of bolt shank in part level, for step 1, pretension values were added, then for the rest steps, bolt lengths were fixed. Other loads were added through reference points, as reference point 1 attached to the surface of column top, reference point 2 corresponded to the surface of column bottom, and reference point 3 linked to beam end. The axial load on column was added at reference point 1 in step 2 and 3, which was a constant value. The beam load was added through altering the displacement at reference point 3 in the loading direction. For constraints of the joint, out-of-plane degrees of freedom were restrained in all the reference points. Reference points 1 and 2 were set as hinge support, in step 2 and 3 the axial displacement of column was released due to the adaptation of the axial load. Reference point 3 only included displacement in loading direction at step 3.

**Table 3** Comparison of ultimate loads from FEM and test results

Group	Axial load ratio	$M_{FEM}/(\text{kN}\cdot\text{m})$	$M_{test}/(\text{kN}\cdot\text{m})$
M16	0.0	43.69	46.03
	0.2	40.87	46.01
	0.4	35.24	45.04
M20	0.0	63.47	53.54
	0.2	36.92	49.72
	0.4	57.89	56.32



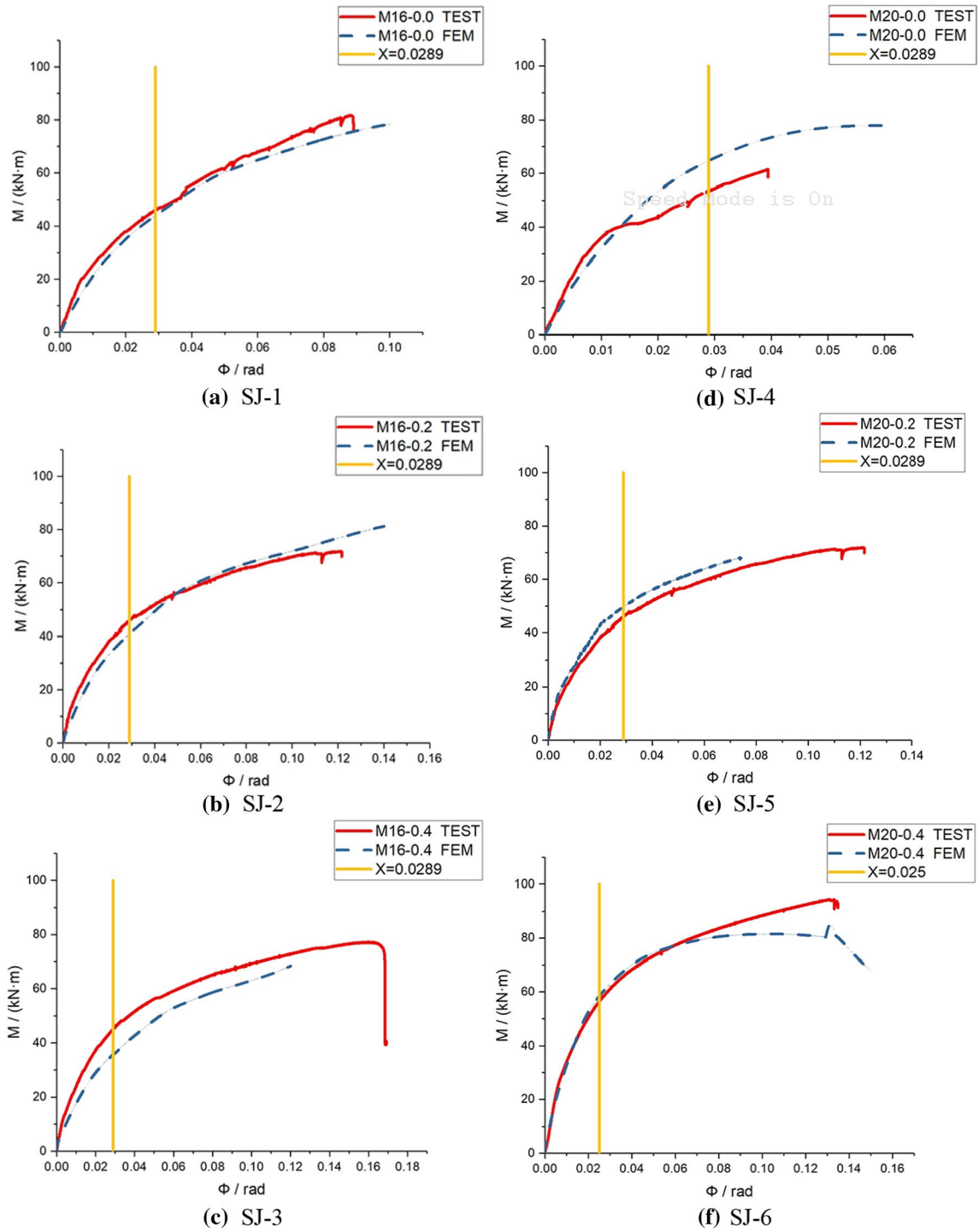


Fig. 7 Comparison of moment-rotation curves

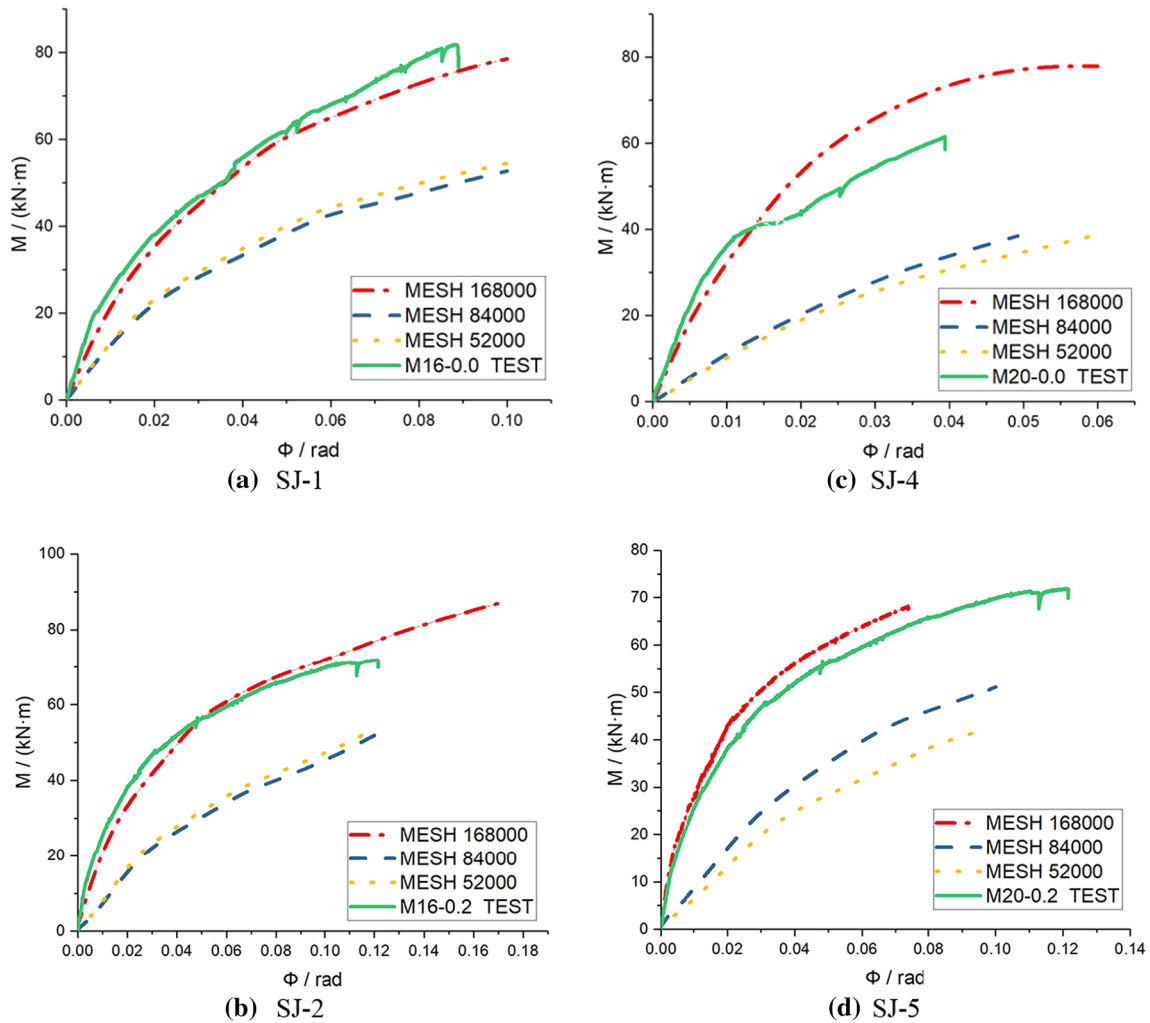


Fig. 8 Comparison of moment-rotation curves in different mesh

## 4.2 Finite Element Results and Discussion

Figure 6c is the contour for one of the joints, where stress pattern and deformation are displayed. Figure 6d is the deformation pattern of the corresponded test, which fits well to the finite element analysis. Figure 6e is the first order mode of column in buckle analysis, as shape is scaled in 300 times. Figure 7 displays the comparison of moment-rotation curves between test and analysis. Table 3 compares the results of ultimate loads in each test.

For some of conditions simulation curves are very closed to the test results. Case SJ-4 (the bolt was M20 and no axial load was applied on column) showed that the curve of test exits a slope mutation at about the angle of 0.01, this is because the test experienced a sudden ground knock from tests elsewhere. For case SJ-3 and SJ-5, results of simulation seems lower than the tests, however the difference is small,

as the slope at the origin which represents initial stiffness is much of the same. Results of finite element analysis can be revealed reliable.

From deformation pattern of tests, it can be concluded that failure mode of joints are yielding of the endplate at first. If loading continues, bolt shanks will bend due to the shear of one-sided bolts until the elliptical heads sheared and damaged. According to the moment-rotation curves of 3 tests on M16 one-sided bolts, as the axial load ratio becomes larger, the ultimate bearing capacity of the joint should decrease slightly. However, as the curves of the 3 tests on M20 one-sided bolts indicated, the ultimate bearing capacity increases when the axial load ratio increases from 0.2 to 0.4, which contradicts the assumption, it is probably because the endplate yielded, which made the capacity not very closely related to the axial load of column.

### 4.3 Mesh Sensitivity Analysis

Mesh sensitivity analysis was done by several groups of models in different grid size as total number of elements were 52,000, 84,000 and 168,000. Both M16 and M20 bolts in axial load ratio of 0.0 and 0.2 were involved in mesh sensitive analysis. In ratio of 0.4 situation, however, most groups of calculation were difficult to converge in step 2, thus were not included.

Comparison of moment–angle curves in different mesh models and the test curve were shown as Fig. 8. As the number of elements decreases, both the ultimate load and the initial stiffness have significant reduction with more deviation from the test. This indicates that the mesh size has great influence on finite element analysis, as the model is more accurate, the result of simulation fit better with the test.

### 5 Conclusion

Through the experiment and finite element analysis of the steel square tubular column and I-shaped steel beam joints which were connected by new elliptical one-sided bolts, the following conclusions can be obtained:

- (1) The failure mode of joints is firstly yielding of the endplate. This means that the joint might be strengthened by increasing thickness of the endplate.
- (2) For M20 group it comes to a pattern that contradicts the expectation about the axial load of the column and ultimate bearing capacity of the joint, as further studies are still need to be carried out.
- (3) With no axial pressure and axial load ratios of 0.2 and 0.4, the ultimate bearing capacity of joints with M20 one-sided bolts increased by 16.32%, 8.06% and 25.04% respectively compared to the beam-column joints with M16 single-sided bolts, which means the capacity of joint can be enhanced by using larger size of new elliptical one-sided bolts.

### References

- CIDECT. (1986). The strength and behaviour of statically loaded welded connections in structural hollow sections, monograph No. 6.
- Elghazouli, A. Y. (2009). Experimental monotonic and cyclic behaviour of blind-bolted angle connections. *Engineering Structures*, 31(11), 2540–2553.
- France, J. E., Buick Davison, J., & Kirby, P. A. (1999a). Strength and rotational response of moment connections to tubular columns using flowdrill connectors. *Journal of Constructional Steel Research*, 50(1), 1–14.
- France, J. E., Buick Davison, J., & Kirby, P. A. (1999b). Moment-capacity and rotational stiffness of endplate connections to concrete-filled tubular columns with flowdrilled connectors. *Journal of Constructional Steel Research*, 50(1), 35–48.
- GB/T2975-2010. (2010). *Steel and steel products—Location and preparation of samples and test pieces for mechanical testing*. Beijing: China Architecture & Building Press. (in Chinese).
- Ghobarah, A., Mourad, S., & Korol, R. (1996). Moment-rotation relationship of blind bolted connections for HSS columns. *Journal of Civil Engineering*, 40(1), 63–91.
- JGJ383-2010. (2010). *Technical specification of lightweight steel and lightweight concrete structures*. Beijing: China Architecture & Building Press. (in Chinese).
- John, J., Charles, G. C., Roy, K., & Lim, J. B. P. (2020a). Performance of a novel slider device in multi-storey cold-formed steel modular buildings under seismic loading. *Structures*, 27, 212–246.
- John, J., Charles, G. C., Roy, K., & Lim, J. B. P. (2020b). Three-storey modular steel building with a novel slider device: Shake table tests on a scaled down model and numerical investigation. *Thin-Walled Structures*, 155, 1–22.
- John, J., Charles, G. C., Roy, K., & Lim, J. B. P. (2020c). Seismic protection of modular buildings with bonded rubber unit sliders: Experimental study. *Thin-Walled Structures*, 154, 1–18.
- John, J., Charles, G. C., Roy, K., & Lim, J. B. P. (2021). Seismic protection of modular buildings with galvanised steel wall tracks and bonded rubber units: Experimental and numerical study. *Thin-Walled Structures*, 162, 1–26.
- Korol, R., Ghobarah, A., & Mourad, S. (1993). Blind bolting W-shape beams to HSS columns. *Journal of Structural Engineering*, 119(12), 3463–3481.
- Lee, J., Goldsworthy, H. M., & Gad, E. F. (2010). Blind bolted T-stub connections to unfilled hollow section columns in low rise structures. *Journal of Constructional Steel Research*, 66(8–9), 981–992.
- Mourad, S., Korol, R. M., & Ghobarah, A. (1996). Design of extended end-plate connections for hollow section columns. *Journal of Civil Engineering*, 23(1), 277–286.
- Pitrakkos, T., & Tizani, W. (2013). Experimental behaviour of a novel anchored blind-bolt in tension. *Engineering Structures*, 49(2), 905–919.
- Ridley-Ellis, D. J. (1998). Fundamental behaviour of rectangular hollow sections with web openings. In *Tubular structures VIII: International symposium on tubular structures*.
- Satasivam, S., & Bai, Y. (2014). Mechanical performance of bolted modular GFRP composite sandwich structures using standard and blind bolts. *Composite Structures*, 117, 59–70.
- Thai, H.-T., & Uy, B. (2015). Finite element modelling of blind bolted composite joints. *Journal of Constructional Steel Research*, 112(2015), 339–353.
- Wan, C., Bai, Y., Ding, C., Zhu, L., & Yang, L. (2020). Mechanical performance of novel steel one-sided bolted joints in shear. *Journal of Constructional Steel Research*, 165, 105815.
- Wang, J., Peng, X., Pan, X., Wang, B., & Zhao, C. (2018b). Pseudodynamic testing of CFST column-to-steel beam frames with high-strength blind-bolted endplate connections. *Journal of Basic Science and Engineering*, 26(5), 11. (in Chinese).
- Wang, J., Zhang, M., & Zhang, Na. (2018a). Experimental and analytical study of the blind bolted end plate steel beam to circular CFDST column joints. *Progress in Steel Building Structures*, 20(2), 36–43. (in Chinese).
- Wang, Z.-Y., & Wang, Q.-Y. (2016). Yield and ultimate strengths determination of a blind bolted endplate connection to square hollow section column. *Engineering Structures*, 111, 345–369.
- Wardenier, J. (2002). *Hollow sections in structural applications*. Bouwen Met Staal.

- Wu, C., Feng, P., & Bai, Y. (2014). Comparative study on static and fatigue performances of pultruded GFRP joints using ordinary and blind bolts. *Journal of Composites for Construction*, *19*, 04014065.
- Yura, J. A., Zettlemoyer, N. A., & Edwards, I. F. (1980). Ultimate capacity equations for tubular joints. In *Proceedings of the annual offshore technology conference*, 3690.

**Publisher's Note** Springer Nature remains neutral with regard to jurisdictional claims in published maps and institutional affiliations.

Springer Nature or its licensor holds exclusive rights to this article under a publishing agreement with the author(s) or other rightsholder(s); author self-archiving of the accepted manuscript version of this article is solely governed by the terms of such publishing agreement and applicable law.